IEEE Photonics Journal
An IEEE Photonics Society Publication

Remotely Pumped All-Optical Wavelength Conversion for WDM-PON-Based Access-Metro Convergence

Volume 13, Number 3, June 2021

Ryota Tsuji
Daisuke Hisano, *Member, IEEE*
Hiroki Takano
Yu Nakayama, *Member, IEEE*
Ken Mishina, *Member, IEEE*
Akihiro Maruta, *Member, IEEE*

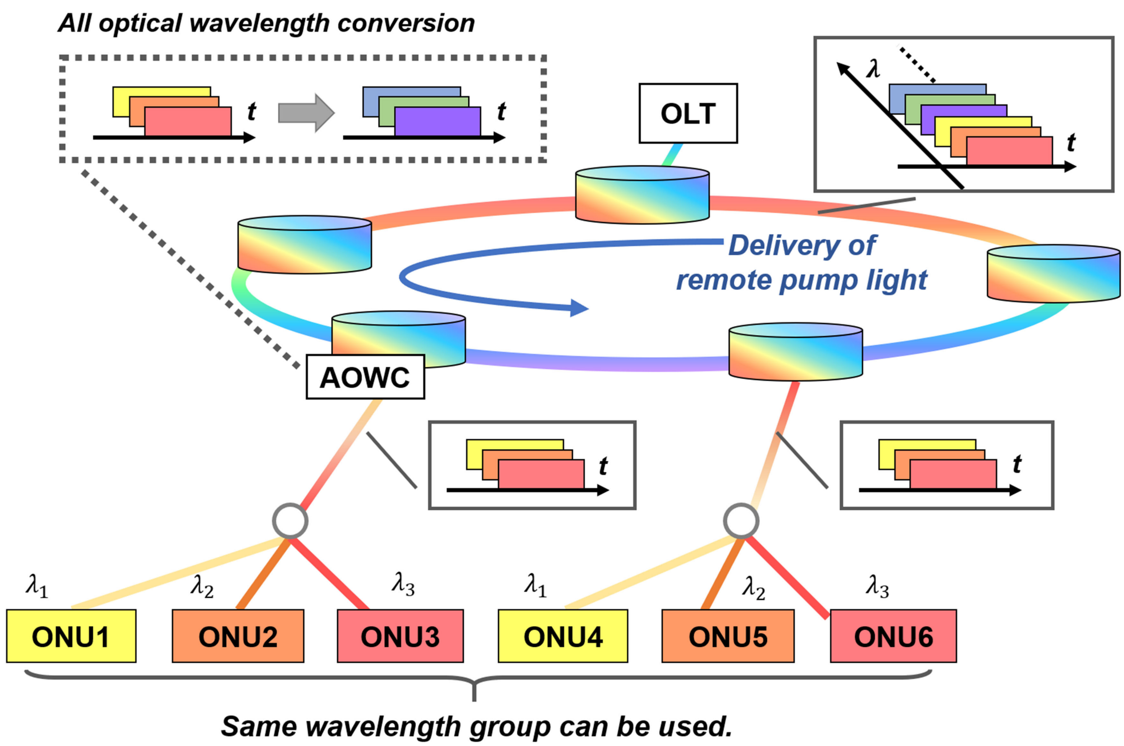

DOI: 10.1109/JPHOT.2021.3071881

IEEE photonics SOCIETY
IEEE

Remotely Pumped All-Optical Wavelength Conversion for WDM-PON-Based Access-Metro Convergence

Ryota Tsuji,[1] Daisuke Hisano ,[1] *Member, IEEE*, Hiroki Takano,[1] Yu Nakayama ,[2] *Member, IEEE*, Ken Mishina ,[1] *Member, IEEE*, and Akihiro Maruta ,[1] *Member, IEEE*

[1] Graduate School of Engineering, Osaka University, Osaka 565-0871, Japan
[2] Institute of Engineering, Tokyo University of Agriculture and Technology, Tokyo 184-8588, Japan

DOI:10.1109/JPHOT.2021.3071881

Manuscript received March 16, 2021; revised March 31, 2021; accepted April 5, 2021. Date of publication April 8, 2021; date of current version April 28, 2021. This work was supported by the Telecommunications Advancement Foundation, Japan, JSPS KAKENHI under Grants JP19K14982 and JP20H04178. This work was presented in part at OECC2020 [7]. Corresponding author: Daisuke Hisano (e-mail: hisano@comm.eng.osaka-u.ac.jp).

Abstract: Access-metro convergence networks (AMCN) have been proposed as a future optical communication network to realize flexible and dynamic bandwidth allocation. An AMCN requires transceivers with different wavelengths for the optical network units (ONUs). This causes an increase in production costs. Although an all-optical wavelength converter (AOWC) mitigates this issue, the AOWC increases the installation cost because it consists of many expensive optical devices. We propose the use of a remotely pumped AOWC (RP-AOWC) with an AMCN. The proposed technique can reduce the number of pump light sources in the AOWC. This paper demonstrates this reduction in the number of light sources and the feasibility of wavelength conversion using pump light propagation. We calculate the reduction in the number of pump sources and the number of transceiver types caused by the use of RP-AOWC and experiment with the wavelength conversion using pump light propagation.

Index Terms: Access network system, passive optical network (PON), bidirectional transmission, interference suppression, wavelength division multiplexing (WDM) scheme.

1. Introduction

Large capacity and low latency optical access networks are commonly in demand to accommodate different user services [1], [2]. Passive optical networks (PONs) are commonly used in optical access networks to efficiently accommodate many users. Each PON system is connected to a metro network consisting of a multi-ring topology. Recently, access-metro convergence networks (AMCNs) have received attention because they can reduce costs by aggregating the optical line terminals (OLTs) on the relay nodes of the metro network to a single node between the metro network and core network [3], [4]. In particular, NTT corporation in Japan has released concept of innovative optical wireless network (IOWN) that aims to realize all-photonic network without electrical and digital signal processing in the middle of end-to-end path [16]. Fig. 1(a) shows the configuration of an AMCN in which a wavelength selective switch (WSS) is installed at each relay node on the metro network instead of the OLT. This configuration achieves low power consumption

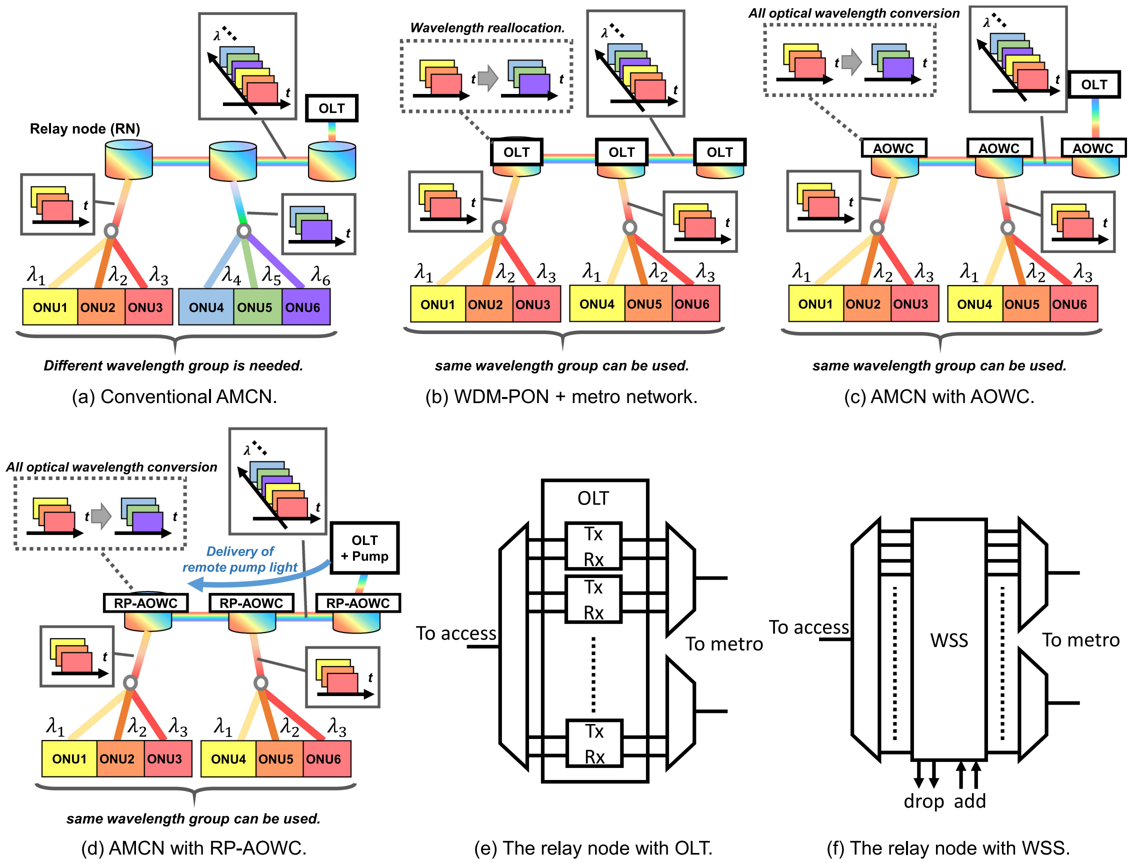

Fig. 1. Comparison of AMCN configurations.

and low latency forwarding because it can connect the access network to the metro network without electrical signal processing. S. Kimura *et al.* [3] found that employing both wavelength-division multiplexing (WDM) and orthogonal frequency division multiplexed (OFDM) schemes with the AMCN can achieve efficient and flexible dynamic bandwidth allocation. In the case of WDM, we must allocate a dedicated wavelength to an optical link between an OLT and an optical network unit (ONU). To avoid wavelength collision on the metro network, all ONUs accommodated in the AMCN must use different wavelengths even if the ONUs are accommodated in different access networks. That is, the AMCN requires as many transceivers with different wavelengths as there are ONUs. Moreover, the coherent transceiver consists of a 90-degree hybrid, high-performance DSP chip, narrow-width laser, and IQ modulator. It is expensive and high-power consumption. The AMCN needs to reduce such a cost.

This paper proposes the use of a novel remotely pumped all-optical wavelength converter (RP-AOWC) with the AMCN system. The proposed technique enables each PON system to use the same wavelength. This is because the relay nodes on the metro ring conduct the AOWC, whereby signals can avoid wavelength collisions on the metro ring network. In particular, using an AOWC is useful in the WDM network because it can convert multiple wavelengths simultaneously using all-optical signal processing [5]. However, because an AOWC uses multiple optical devices, the cost benefit decreases. Employing an RP-AOWC can reduce the number of pump light sources compared with the conventional AOWC owing to the aggregation of the pump light sources into a relay node where the OLT is installed. The effects of remotely pumped light on the performance of wavelength conversion and simultaneous transmission of signals have been reported in [6] using numerical simulations.

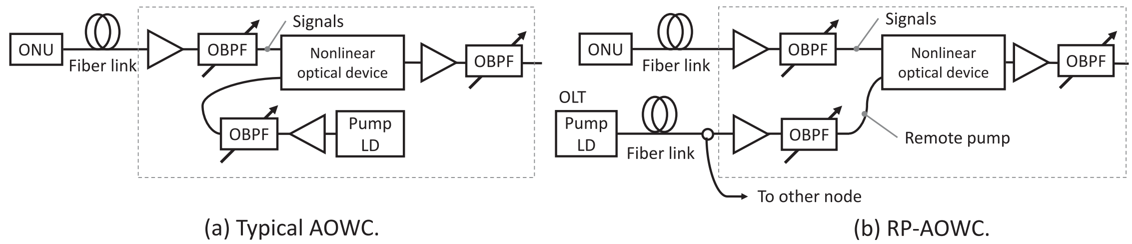

Fig. 2. The configuration of all-optical wavelength converter without and with remotely pump.

This paper reports an analysis of the reduction in the number of transceiver types and that of pump light sources when applying the proposed RP-AOWC to an AMCN. Moreover, we experimentally demonstrate the feasibility of the RP-AOWC. Note that this paper is an expanded version of the previous work reported in OECC2020 [7]. All data have been updated. Additionally, detailed conditions were set for the analysis of the reduction, an auto-tracking polarization controller (APC) was introduced for the experiment, and two-stage wavelength conversion was performed. The remainder of this paper is organized as follows. Section II presents the concept of RP-AOWC and describes our contributions. In section III, we calculate the reduction in the number of transceiver types and that of the pump light sources by solving an optimization problem. The experimental results of employing the RP-AOWC, are reported in Section IV. The conclusions of this study are provided in section V.

2. Principle of RP-AOWC for AMCN

This section describes the principles of the operation and our contributions. First, we explain the concept of the proposed method. After that, we describe the study's contributions.

2.1 Concept

Fig. 1(a), (b), (c) and (d) show conventional AMCN, the WDM-PON and metro network, AMCN with ordinary AOWCs, and AMCN with proposed RP-AOWCs, respectively. In a typical case, each OLT is installed in each relay node and connected to the ONUs as shown in Fig. 1 (e). The AMCN aggregates OLTs to a boundary node between the metro network and the core network. Fig. 1 (f) shows the WSSs are installed at the relay nodes. The WSS-based signal forwarding can reduce the transmission delay and power consumption because the optical signals can pass through the relay node without electrical processing. However, the WDM-based AMCN must allocate different wavelengths to each ONU even if ONUs are accommodated in a different PON system. Therefore, the AMCN requires the installation of transceivers with different wavelengths in the ONUs. As shown in Fig. 1 (c), installing AOWCs in relay nodes reduces the number of transceiver types. Each PON link in access link can use the same wavelength group. When the signals coming from access links are input into metro network, the AOWC can change the wavelength group and avoid wavelength collision on the metro ring network. AOWC conducts all-optical processing to eliminate electrical signal processing from the relay nodes. Moreover, it can convert multiple wavelength channels simultaneously. While the signals coming to the AOWC have random polarization rotation, polarization insensitive wavelength convertor has been reported and can corresponds with this problem [11], [12], [17]–[19]. Thus, the AMCN with the AOWC achieves flexible dynamic bandwidth allocation. Meanwhile, the AOWC system consists of optical amplifiers such as an erbium-doped fiber amplifier (EDFA), nonlinear devices such as a highly nonlinear fiber (HNLF), optical bandpass filters (OBPFs), and wavelength-tunable light sources for the pump light as shown in Fig. 2. These components increase the installation cost of the AOWC.

The proposed RP-AOWC mitigates this issue. As shown in Fig. 1 (d), when using this scheme, pump light sources are not installed in most AOWCs. The pump light sources are installed in some of the relay nodes and are shared with other relay nodes without pump light sources. According to demand, the nodes with the pump sources transmit the pump light to the nodes without the pump light sources. When multiple nodes require pump light of the same wavelength simultaneously, a single light source is sufficient for the proposed method. In other words, the RP-AOWC can satisfy the wavelength conversion requirement with a smaller number of light sources than the conventional AOWC, resulting in a reduction in the installation cost of the AOWC.

The proposed AOWC can also be used for coexistence with conventional (legacy) PONs. However, since there are some cases where the link budget is insufficient, signal regeneration and modulation format conversion are required. These functions can be realized as all-optical signal processing [21]–[24].

2.2 Contribution

This paper proposes utilizing the RP-AOWC with the AMCN. The proposed scheme can reduce the following quantities:

1) The number of transceiver types installed in ONUs,
2) The number of light sources for pump light used for the AOWC.

Regarding the first item, note that the proposed scheme does not aim to reduce the total number of transceivers. Rather, it enables the production cost to be reduced because transceivers with the same wavelengths can be prepared even for different PON systems. Regarding the second item, the use of an RP-AOWC can reduce the total number of pump light sources because the light sources are installed in some of the relay nodes, and most relay nodes share light sources. In particular, because the typical AOWC requires expensive light sources with narrow linewidths, the RP-AOWC scheme can significantly contribute to cost reduction. Here, the proposed RP-AOWC is pointed out that the RP-AOWC must install an optical amplifier in the relay node to amplify pump lights transmitted from the OLT. That is, the cost reduction cannot be achieved. However, typical AOWCs also require installing an optical amplifier to amplify pump lights. Thus, the proposed RP-AOWC does not change the total number of EDFAs compared to the typical AOWC [11]. The OLT aggregating pump light sources need to install an optical amplify but require one optical amplifier because the amplifier can amplify multiple pump lights simultaneously. Besides, since the pump light is a continuous wave (CW) one, we can use a semiconductor optical amplifier (SOA) instead of EDFA.

The contributions of this study are as follows:

1) To estimate the effect of the proposed method, we calculated the reduction in the light sources for the pump lights of the RP-AOWC compared with those of the typical AOWC.
2) To investigate the feasibility of the RP-AOWC in AMCNs, we conducted a proof-of-concept experiment.

The following sections explain these contributions.

3. Analysis of Reduction in Number of Light Sources

This section presents the analytical results of reducing the number of pump sources used in the RP-AOWC and the transceiver types in the ONUs. The number of transceiver types in the proposed scheme is calculated in Section III-A. Section III-B shows the reduction in the number of pump sources.

3.1 Reduction in Number of Transceiver Types in ONUs

We calculated the number of transceiver types in the conventional AMCN and AMCN with AOWC. Note that there is no difference in the total number of transceivers between the AOWC and RP-AOWC. Thus, we compared the AOWC case with the conventional AMCN case. For the conventional AMCN case, the total number of transceiver types is $N_a \times N_d$, where N_a is the maximum number of ONUs in each PON system, and N_d is the number of relay nodes in the metro ring network. This is because the ONUs have to use different wavelengths on the AMCN even when each ONU is accommodated in a different access branch link. As the size of the metro ring increases, the number of transceivers increases. For the AOWC-based AMCN, the wavelength allocation in each access system can be determined independently because the wavelength of the signal is converted into another wavelength when the signal is input into the metro ring network. Therefore, the total number of transceiver types is N_a. This result contributes to a significant reduction in cost.

3.2 Reduction in Number of Pump Sources

3.2.1 Optimization Problem: The signals propagate through the AMCN from the ONUs to the OLT. In this case, the AOWC converts the signal wavelengths into other wavelengths to avoid signal collisions. The proposed RP-AOWC can reduce the number of pump light sources. This section estimates the number of pump light sources that can be reduced. Therefore, to estimate the minimum number of pump light sources when given the number of relay nodes on the AMCN, we solve the following optimization problem,

$$\min \sum_{P} x_i, \tag{1}$$

where $x_i = \{0, 1\}$ is the reservation status of a frequency slot. When $x_i = 1$, the slot is reserved. Each slot does not accept reservations from two or more signals to avoid signal collision. In other words, one signal occupies one slot. $P \in \{x_i | i \in n(N_a + 1), n \in \mathbb{Z}\}$ is a subset of the set $X \in \{x_i | i \in \mathbb{Z}\}$ of frequency slots. i is the frequency slot identifier. P is the subset of the frequency slot used for the pump light. In other words, the objective function indicates the minimization of the number of pump light sources. In this section, the constraints are described. In the FWM process, a fourth light is generated when a signal light and two pump lights are input into a nonlinear medium. The new frequency f_{i+j-k} of the wavelength-converted light is expressed as:

$$f_{i+j-k} = f_i + f_j - f_k, \tag{2}$$

where f is the frequency of the light, i, j, k are the frequency slot identifiers, and $i, j \neq k$. When $i = j$, the FWM is called a degenerate FWM. Note that this analysis uses both degenerate and non-degenerate FWM processes. The next condition concerns the maximum interval of the frequency slot between lights when using FWM as follows:

$$c_{i,j} |i - j| \leq D_p, \tag{3}$$

where D_p is the maximum interval of the frequency slot when using FWM and $c_{i,j} \in \{0, 1\}$ is the availability of a pair of light sources. $c_{i,j} = 1$ implies that the AOWC uses the frequency slots i and j. The available frequency range of the AOWC is determined by

$$f_{\min} \leq f_i \leq f_{\max}, \tag{4}$$

where $f_{\max}$ and $f_{\min}$ are the upper and lower limits of the communicable band, respectively. The RP-AOWC-based AMCN conducts a multistage AOWC. In other words, the wavelength of the signals is converted into other wavelengths at multiple relay nodes. Thus, we must limit the maximum number of stages of the wavelength conversions as follows:

$$r_m \leq L, \tag{5}$$

where r_m is the number of stages of the wavelength conversion at m, and L is the maximum number of stages of the wavelength conversion for a signal. Finally, we provide the constraint to determine whether all signals can be allocated to the frequency slot:

$$\sum_{S} x_i = N_a N_d, \tag{6}$$

TABLE 1
Variables

Variable	Definition
i, j, k	Frequency slot identifier
$m \in \mathbb{N}$	Relay node identifier
$x_i \in \{0, 1\}$	Reservation status of frequency slot
$r_m \in \mathbb{N}$	No. of stages of wavelength conversion at node m
$c_{i,j} \in \{0, 1\}$	The availability of pair of light sources, $i \neq j$
$f_i \in \mathbb{R}$	Frequency at i
$f_{max} \in \mathbb{R}$	Upper limit of communicable band
$f_{min} \in \mathbb{R}$	Lower limit of communicable band
$D_p \in \mathbb{N}$	Maximum interval of frequency slot when using FWM
$L \in \mathbb{N}$	Maximum No. of AOWC for signal
$N_a \in \mathbb{N}$	Maximum No. of ONUs in PON system
$N_d \in \mathbb{N}$	No. of relay nodes

where $S = X \backslash P$ denotes a set of signal lights. If this condition is not satisfied, all ONUs cannot be accommodated, and communication is not possible. As an initial state, x_i is set as follows:

$$x_i = \begin{cases} 1, & i = \{1, 2, 3, \ldots, N_a\} \\ 0. & \text{otherwise} \end{cases} \tag{7}$$

This initial condition is necessity because the ONUs can use the same wavelength among the different access networks. That is, these initial wavelengths are used in all access networks. Table 1 summarizes these variables.

3.2.1 Analysis Results: Under the aforementioned constraint, the parameter that affects the signal quality is D_p because the frequency interval in FWM is directly related to the conversion efficiency. A large frequency interval leads to a decrease in the OSNR of the wavelength-converted light. Therefore, we calculated certain patterns by varying D_p. The number of relay nodes N_d is also an important parameter. The maximum value of N_d was set to 24 because 8 nodes can be accommodated in the C-band and 16 nodes can be accommodated in the L-band, considering that the bandwidth of the signal light in a PON system is 400 GHz when the bandwidth per slot is 50 GHz [10]. D_p was set to up to 53 slots ($\approx$ 2650 GHz) [11], taking into account the degradation of the pump light caused by transmission. f_{max} and f_{min} were set to 195.942 THz and 184.487 THz to accommodate the C- and L-bands. As fixed parameters, we set $N_a = 8$ and $L = 2$. This is because ITU-T G.989.2 determined the typical maximum number of ONUs to be 8 [13]. For L, multistage conversion distorts the signal. The number of wavelength conversions for a signal should be lower. Thus, we set a small value for L. Note that there is no constraint on the wavelength of the pump light for the conventional AOWC.

Fig. 3 shows the calculation result. The number of relay nodes does not reach 24 in some figures because D_p limits the number of wavelength slots that can be allocated by wavelength conversion. The brown line shows the results from the RP-AOWC based on the optimization problem, as shown in the previous section. The gray line shows the result of employing the typical AOWC. The larger the maximum frequency interval D_p, the smaller the number of pump sources required. Since the minimum number of pump light sources is 2 for $N_d = 8$ and 6 for $N_d = 24$, the reduction ratio of pump light sources is 71% for $N_d = 8$ and 75% for $N_d = 24$.

In this case, we assumed the metro link consists of two cables of optical fibers in the optimization. In other words, the uplink and downlink are split physically. Note that when both uplink and downlink signals are shared as a single optical fiber, the wavelength bandwidth has to be divided in half, and the required pump sources are doubled.

These results indicate that RP-AOWC is a technique that can significantly reduce the number of pump light sources compared with the conventional AOWC.

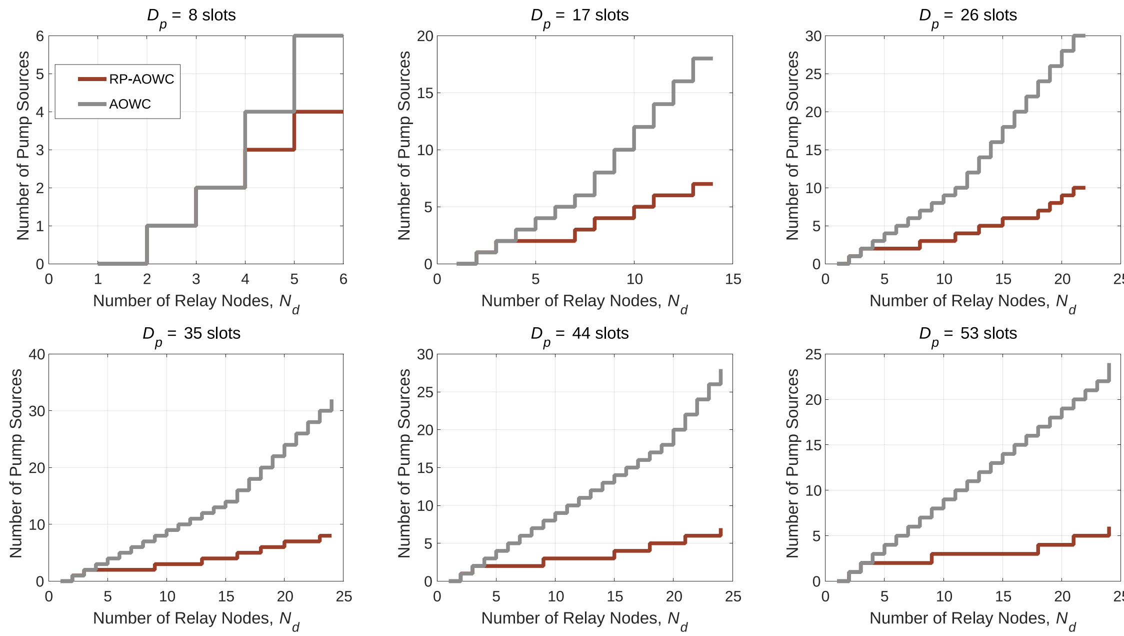

Fig. 3. Number of pump light sources when changing number of relay nodes.

4. Experiments

In this section, we investigate the feasibility of the proposed scheme. We conducted experiments with an RP-AOWC.

4.1 Experimental Setup

Three types of experiments were performed. Fig. 4(a) shows the configuration of the back-to-back system. Fig. 4 (b) shows the configuration of a pump propagating a standard single-mode fiber (SSMF) employing an RP-AOWC. Fig. 4 (c) shows a two-stage wavelength conversion with the RP-AOWC. The proposed RP-AOWC can reduce the number of pump sources more efficiently when multistage wavelength conversion among several relay nodes is allowed. In this experiment, we obtained the bit error rate (BER) of wavelength-converted light to investigate the impact of the fiber transmission of the pump light on the wavelength conversion characteristics. The experimental conditions are as follows. At the transmitter side, a bit sequence was generated and set to a pseudo-random bit sequence with a length of $2^{15} - 1$. The bit sequence was modulated to a quadrature phase-shift keying (QPSK) signal. After modulation, the signal passed through an RRC filter with a roll-off ratio of 0.2. The filtered signal was 2-fold upsampled. After upsampling, the signal was resampled to 12 GSa/s to match the sampling rate of an arbitrary waveform generator (AWG), AWG 7122C released by Tektronix, Inc. The signal light wavelengths were set to 1556 nm or 1552 nm for one-stage conversion and 1556 nm for two-stage conversion. The average optical power of the signal light was adjusted to 0 dBm and input into the HNLF. The wavelengths of the pump light were set to 1554 nm and 1550 nm, respectively. We used several light sources. The light source linewidth was 5 kHz in the 1554-nm wavelength case and 1 kHz in the 1550-nm case.

The propagation distance of the pump light was set to 60 km because metro ring networks frequently have distances of several dozen kilometers. In the two-stage conversion, these pump lights propagated through the same fiber. For comparison, we also experimented with the case of no transmission. The pump light after SSMF propagation was amplified to 10 dBm by EDFA and input into the HNLF. We adjusted the power of the pump light to the value at which Brillouin backscattering light is not generated [9]. In the case of two-stage conversion, the pump light

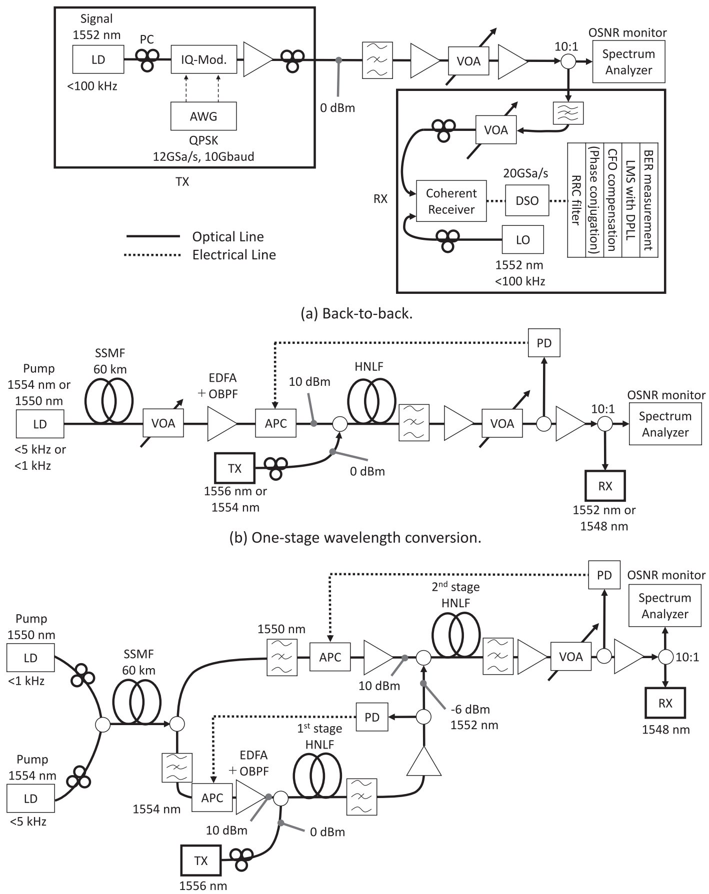

Fig. 4. Experimental setups.

TABLE 2
The Fiber Parameters

		1st stage		2nd stage	
	SSMF	HNLF1	HNLF2	HNLF3	HNLF4
Chromatic dispersion [ps/nm/km]	17	0.62	−0.32	0.57	−0.8
Third-order dispersion $[\mathrm{ps/nm^2/km}]$	N/A	0.027	0.025	0.027	0.031
Nonlinear coefficient $[\mathrm{W}^{-1}$/km]	2	13	13	13	12
Fiber loss [dB/km]	0.2	0.56	0.56	0.54	0.51
Fiber length [km]	60	0.5	0.535	0.72	0.82

before amplification is extracted by the OBPF and then amplified. The wavelength-converted light output from the HNLF was extracted using another OBPF. In the two-stage conversion, the wavelength-converted light was amplified to −6 dBm by EDFA and then input into the second HNLF. To generate the high-quality wavelength-converted signal in the HNLF, we introduced an APC. The APC adjusted the polarization state to maximize the power of the wavelength-converted light. That is, the APC ensures that the polarization of the signal light and pump light match. The parameters of SSMF and HNLF are summarized in Table 2. We used HNLF1 and HNLF2 in the first stage and HNLF3 and HNLF4 in the second stage.

At the receiver side, the wavelength-converted light was received and sampled by a digital storage oscilloscope (DSO) X95004Q, released by Keysight Technologies with 20 GSa/s and 8 GHz in the analog bandwidth, and digital signal processing (DSP) was performed offline. The key functions of the DSP are as follows: First, the signal is received by the RRC filter. Next, the signal was

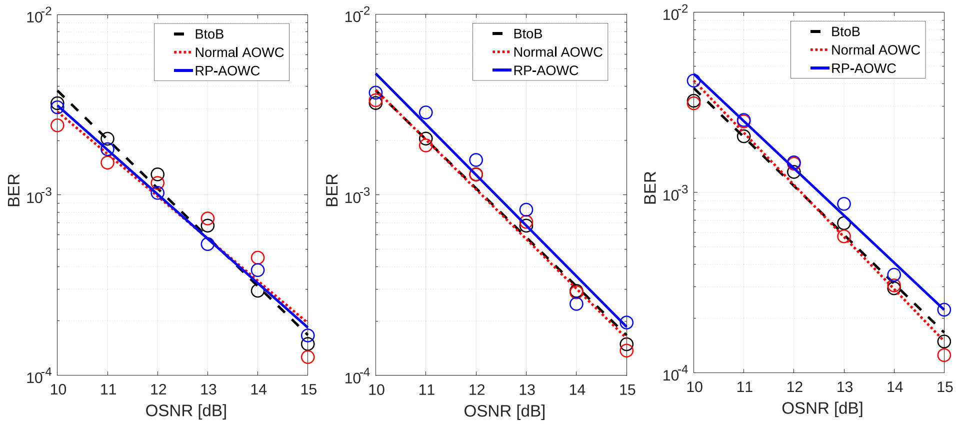

1556 nm to 1552 nm. 1552 nm to 1548 nm. Two-stage conversion.

Fig. 5. BER of wavelength converted signal.

subjected to phase conjugation for the wavelength-converted signal and coarse carrier frequency offset compensation was performed in the frequency domain [15]. Symbol synchronization was performed by equalizing the received signal with an adaptive equalizer employing a constant modulus algorithm (CMA). After the CMA-based equalizer, the DSP conducted cross-correlation between the pilot sequence in the equalized signal with the training data sequence. After adjusting the symbol timing between the signal and the training data sequence, the DSP applied a least mean square (LMS)-based equalizer with a digital phase-locked loop (PLL) in the time domain [8]. The equalizers consisted of a finite impulse response (FIR) filter. For the FIR filter parameters, the tap factor, step size, and number of training symbols were 9, 0.004, and 3000, respectively. The optimal value of the loop gain of the filter was determined using a full-search algorithm.

4.2 Experiment Results

Fig. 5(a), (b) show the results of one-stage wavelength conversion for 1556 nm to 1552 nm and 1552 nm to 1548 nm, respectively. Fig. 5 (c) shows the results of two-stage wavelength conversion. We drew approximate lines based on the least-squares method. The dashed black line is the result of the back-to-back transmission, the dotted red line is the BER line of the wavelength conversion without remote pumping, and the solid blue line is the BER of the remotely pumped wavelength conversion with 60-km propagation of the pump light.

We used the black line as a benchmark. The OSNR penalty is less than 0.5 dB for all results at BER $= 3.8 \times 10^{-3}$ at output BER $= 10^{-13}$ which is the hard-decision forward error correction (HD-FEC) limit [14]. From these results and the fact that the pump light is continuous, we consider that the main factor causing this penalty is the lower conversion efficiency caused by the polarization fluctuation. The APC monitors the average optical power of the wavelength-converted light to adjust the polarization of the pump light. The feedback configuration can obtain this monitored power so that a feedback delay occurs. Furthermore, we can achieve error-free operation with a small OSNR penalty compared with that of back-to-back transmission. These results imply that RP-AOWC has little effect on the quality of the signal in the AMCN.

5. Conclusion

This paper proposes utilizing an RP-AOWC with the AMCN. The proposed technique reduces the number of transceiver types in the ONU and the number of pump light sources in the AOWC. Consequently, the technique can reduce the production cost of the ONU and the cost of the AOWC. First, we calculated the reduction in the light source. The number of transceiver types was the maximum number of ONUs in the PON system, regardless of the number of relay nodes. The number of pump light sources was reduced by 71% when the number of relay nodes in the AMCN was 8. Next, to confirm that the RP-AOWC can be used in AMCN, we conducted experiments with two-stage wavelength conversion for a 20-Gbps QPSK signal with pump light propagating through the SSMF. When the propagation distance of the pump light was 60 km, the OSNR penalty of the wavelength-converted signal was less than 0.5 dB at the HD-FEC limit. Moreover, the BER values were below the FEC limit in OSNR $\geq$ 11 dB. Therefore, the transmission of the pump light has little effect on wavelength conversion. In conclusion, the application of the RP-AOWC to an AMCN is feasible and effective for cost reduction. Because the main subject of this paper is to investigate the feasibility of applying the RP-AOWC, we did not do the following, the feasibility of the proposed method will be further enhanced by conducting experiments on the transmission of polarization multiplexing and WDM signals.

References

[1] N. Iiyama, M. Fujiwara, T. Kanai, J. Kani, and J. Terada, “The approaches of coherent technology for TDM-PON,” in *Proc. 45th Eur. Conf. Opt. Commun.*, Sep. 2019, pp. 1–3.

[2] F. J. Effenberger, “PON standardisation status and future prospects,” in *Proc. 45th Eur. Conf. Opt. Commun.*, Paper M.2.F.1, Sep. 2019, pp. 1–3.

[3] S. Kimura, “Elastic lambda aggregation network (E λ AN)-Proposal for future optical access network,” in *Proc. 18th Optoelectron. Commun. Conf. Held Jointly Int. Conf. Photon. Switching*, 2013, pp. 1–2.

[4] T. Kanai *et al.*, “Novel automatic service restoration technique by using self-reconfiguration of network resources for a disaster-struck metro-access network,” *J. Lightw. Technol.*, vol. 36, no. 8, pp. 1516–1523, Apr. 2018.

[5] S. Namiki, K. Solis-Trapala, H. N. Tan, M. Pelusi and T. Inoue, “Multi-channel cascadable parametric signal processing for wavelength conversion and nonlinearity compensation,” *J. Lightw. Technol.*, vol. 35, no. 4, pp. 815–823, Feb. 2017.

[6] R. Tsuji, D. Hisano, K. Mishina, and A. Maruta, “Remote pumped all optical wavelength converter for metro-core photonic networks,” *IEICE Trans. Commun.*, vol. 103, no. 11, pp. 1282–1290, 2020.

[7] R. Tsuji, D. Hisano, Y. Nakayama, K. Mishina, and A. Maruta, “Remote-pumped all-optical wavelength conversion for WDM-PON-based access-metro convergence,” in *Proc. Opto-Electron. Commun. Conf.*, Paper VP86, 2020, pp. 1–3.

[8] T. Kobayashi *et al.*, “160-Gb/s polarization-multiplexed 16-QAM long-haul transmission over 3123 km using digital coherent receiver with digital PLL based frequency offset compensator,” in *Proc. Conf. Opt. Fiber Commun.*, 2010, pp. 1–3.

[9] G. Agrawal, *Nonlinear Fiber Optics*, 5th ed. New York, NY, USA: Academic Press, 2013.

[10] ITU-T G. 692, “Optical interfaces for multichannel systems with optical amplifiers,” 1998.

[11] T. Inoue, K. Tanizawa, and S. Namiki, “Guard-band-Less and polarization-insensitive tunable wavelength converter for phase-modulated signals: Demonstration and signal quality analyses,” *J. Lightw. Technol.*, vol. 32, no. 10, pp. 1981–1990, May 2014.

[12] T. Inoue, S. Takasaka, K. Ota, and S. Namiki, “Design and demonstration of 30-nm tunable guard-band-less all-optical wavelength converter for WDM signals,” in *Proc. Opt. Fiber Commun. Conf. Exhib.*, 2017, pp. 1–3.

[13] ITU-T G.989.2, “40-Gigabit-Capable Passive Optical Networks 2 (NG-PON2),” 2013.

[14] ITU-T G.975.1, Appendix I.9, “Forward Error Correction for High Bit-Rate DWDM Submarine Systems,” 2004.

[15] T. Nakagawa *et al.*, “Non-data-aided wide-range frequency offset estimator for QAM optical coherent receivers,” in *Proc. Opt. Fiber Commun. Conf. Expo. Nat. Fiber Optic Engineers Conf.*, 2011, pp. 1–3.

[16] IOWN Grobal Forum. Online [Available]: https://iowngf.org

[17] J. Lu, L. Chen, Z. Dong, Z. Cao, and S. Wen, “Polarization insensitive wavelength conversion based on orthogonal pump four-wave mixing for polarization multiplexing signal in high-nonlinear fiber,” *J. Lightw. Technol.*, vol. 27, no. 24, pp. 5767–5774, Dec. 2009.

[18] S. Takasaka, M. Takahashi, Y. Mimura, M. Tadakuma, R. Sugizaki, and T. Yagi, “Polarization insensitive arbitrary wavelength conversion in entire c-band using a PM-HNLF,” in *Proc. 36th Eur. Conf. Exhib. Opt. Commun.*, 2010, pp. 1–3.

[19] M. A. Ettabib *et al.*, “Polarization insensitive wavelength conversion in a low-birefringence SiGe waveguide,” *IEEE Photon. Technol. Lett.*, vol. 28, no. 11, pp. 1221–1224, Jun. 2016.

[20] H. N. Tan *et al.*, “On the cascadability of all-optical wavelength converter for high-order QAM formats,” *J. Lightw. Technol.*, vol. 34, no. 13, pp. 3194–3205, Jul. 2016.

[21] A. E. Willner, S. Khaleghi, M. R. Chitgarha, and O. F. Yilmaz, “All-optical signal processing,” *J. Lightw. Technol.*, vol. 32, no. 4, pp. 660–680, Feb. 2014.

[22] M. Matsumoto, “Fiber-based all-optical signal regeneration,” *IEEE J. Sel. Topics Quantum Electron.*, vol. 18, no. 2, pp. 738–752, Mar.-Apr. 2012.

[23] K. Mishina *et al.*, “NRZ-OOK-to-RZ-BPSK modulation-format conversion using SOA-MZI wavelength converter,” *J. Lightw. Technol.*, vol. 24, no. 10, pp. 3751–3758, Oct. 2006.

[24] K. Mishina, S. Kitagawa, and A. Maruta, “All-optical modulation format conversion from on-off-keying to multiple-level phase-shift-keying based on nonlinearity in optical fiber,” *Opt. Exp.*, vol. 15, no. 13, pp. 8444–8453, 2007.